



Published in final edited form as:

Nat Neurosci. 2019 September ; 22(9): 1460–1468. doi:10.1038/s41593-019-0444-x.

A neural heading estimate is compared with an internal goal to guide oriented navigation

Jonathan Green^{1,2}, Vikram Vijayan¹, Peter Mussells Pires¹, Atsuko Adachi¹, Gaby Maimon^{1,*}

¹Laboratory of Integrative Brain Function and Howard Hughes Medical Institute, The Rockefeller University, New York, New York, USA.

²Present address: Department of Neurobiology, Harvard Medical School, Boston, Massachusetts, USA.

Abstract

Goal-directed navigation is thought to rely on the activity of head-direction cells, but how this activity guides moment-to-moment action remains poorly understood. Here we characterize how heading neurons in the *Drosophila* central complex guide moment-to-moment actions. We establish an innate, heading-neuron dependent, tethered navigational behavior where walking flies maintain a straight trajectory along a specific angular bearing for hundreds of body lengths. While flies perform this task, we use chemogenetics to transiently rotate their neural heading estimate and observe that the flies slow down and turn in a direction that aims to return the heading estimate to the angle it occupied prior to stimulation. These results support a working model in which the fly brain quantitatively compares an internal estimate of current heading with an internal goal heading and uses the sign and magnitude of the difference to determine which way to turn, how hard to turn, and how fast to walk forward.

Introduction

Fruit bats return to the same fruit tree night after night¹ and desert ants walk straight back to their nest after long, meandering foraging runs². How do nervous systems mediate such navigational behaviors?

In mammals, correlative neurophysiological experiments have revealed the existence of head-direction cells: neurons whose firing rates co-vary with the animal's head angle in the

Users may view, print, copy, and download text and data-mine the content in such documents, for the purposes of academic research, subject always to the full Conditions of use:http://www.nature.com/authors/editorial_policies/license.html#terms

*Corresponding author: maimon@mail.rockefeller.edu.

Author Contributions

J.G., V.V., and G.M. conceived the project. J.G. performed two-photon imaging and stimulation experiments. P. M.-P. performed purely behavioral experiments in plate-tethered wild-type and *shibire*-impaired flies. G.M. and J.G. performed behavioral experiments in pin-tethered flies. J.G., V.V., P.M.-P. and G.M. analyzed and interpreted experiments. V.V. developed the bar jump perturbation approach for studying goal-directed walking. A.A. performed and analyzed multi-color-flip-out anatomical experiments. J.G. and G.M. wrote the paper.

Competing Interests Statement

The authors declare no competing financial interests.

world³. More recent experiments have also revealed the existence of heading-sensitive cells in insects^{4,5}, including *Drosophila*⁶. Beyond heading cells, neurons signaling the animal's heading relative to a goal location were recently discovered in the bat hippocampus⁷. A natural assumption is that such heading- and heading-relative-to-goal signals govern moment-to-moment actions during navigational tasks, but direct perturbational evidence for this idea has been lacking.

When considering how to experimentally determine how, for example, heading cell activity guides moment-to-moment navigational actions, one is confronted with the fact that heading cell activity may both control and be controlled by the animal's angular heading, raising a fundamental challenge in dissociating cause and effect in the system. One way to address this challenge is to break the feedback loop by manipulating the heading signal to an experimentally chosen angular value during navigation. Because when it is momentarily under experimental control the heading signal cannot be updated by the animal's own actions, this manipulation allows one to determine how heading-cell activity guides navigational turns and forward velocity independently of how the same signal is updated by these actions. Although inactivation experiments that degrade (as opposed to coherently rotate) head-direction cell activity in rodents⁸ and heading-cell activity in flies⁹ have demonstrated that heading signals are generally required for observing straight, goal-oriented, trajectories, these perturbations have not allowed one to differentiate among models for precisely how the activity of these cells influences the animal's moment-to-moment actions during navigation.

To transiently rotate a population-level heading signal in a navigating animal, we first establish a goal-directed navigational behavior in tethered, walking *Drosophila*. One way to study goal-directed navigation is to train an animal to navigate to a defined spatial location in an environment, as has been done with flying bats trained to land on a perch⁷. In this scenario, one can assume that the animal, at most moments during its trajectory, is trying to make its way to a specific 2D or 3D goal location. In our case, we did not train the flies to navigate to a virtual 2D or 3D goal location. Instead, we focused on an innate behavior in which flies walk forward for meters while maintaining a consistent angular bearing relative to a visual landmark (also called menotaxis in flying *Drosophila*¹⁰), with no clear aim to reach any specific 2D or 3D location. While this behavior represents a very simple navigational task, maintaining a consistent angular bearing relative to visual landmarks is likely to be an essential sub-task in other navigational trajectories, like those that are clearly aimed at reaching specific 2D or 3D locations. Moreover, this innate behavior on the ball resembles other, ethologically important, dispersal behaviors in which animals walk along nominally straight trajectories for minutes or hours at a time, with no explicit 2D or 3D positional goal¹¹.

After demonstrating that this oriented dispersal behavior in *Drosophila* requires normal-functioning heading neurons—consistent with past reports on other orienting behaviors^{8,9}—we leverage the anatomical organization of the fly heading system to stimulate heading cells tuned to the same preferred heading angle, inducing the population-level heading estimate carried by heading neurons to naturalistically rotate in flies performing the task. We show that in response to having their internal heading estimate rotated, flies quickly turn in a

direction that aims to bring the heading estimate back toward the value it occupied prior to stimulation. We also show that flies slow down their forward walking speed after heading-signal rotations, a behavioral reaction which likely serves to minimize displacements in the “wrong” direction. Along with other purely behavioral experiments, these results support a model in which the fly brain quantitatively compares a population-level estimate of current heading with an internal goal to guide the animal’s turning and forward-walking velocities.

Results

Flies can maintain their walking direction at arbitrary angles

To study how *Drosophila*’s heading system guides navigational behavior in a controlled setting, we placed tethered flies on an air-supported ball¹²⁻¹⁴ at the center of a cylindrical LED arena¹⁵, and presented them with a bright vertical bar whose position on the LED display rotated in closed-loop with the fly’s yaw (left/right) rotations on the ball. This closed-loop condition simulates the fly walking in a visually barren landscape with a single stable landmark located very far away, at visual infinity (like the moon), which the flies can use for inferring their angular orientation^{14,16} (Figure 1a). To promote robust walking, we studied food-deprived flies heated to 34°C, conditions that likely motivated dispersal from the current (virtual) location. Under these conditions, we found that, without training, flies walked forward on the ball for hundreds of body-lengths while maintaining a relatively stable angular bearing relative to the vertical bar (Figure 1b). The specific angle at which each fly stabilized the bar differed across individuals. Single flies also spontaneously changed the stable heading they kept in relation to the bar, either abruptly or gradually over time.

To quantify these data, we treated each 20-ms angular heading measurement in a walking fly as a unit vector, computed the mean of unit vectors over 60 s windows (Figure 1c), and visualized the distribution of 60-s mean vectors over the hour-long experiment in a polar plot (Figure 1d, see Supplementary Figure 1 for Methods). As expected from the virtual 2D trajectories (Figure 1b), these polar plots revealed flies to be walking in a relatively constant direction with respect to the bar over one-minute-long time windows (data points near the edge of the circle, Figure 1c-d).

Because we performed hour-long behavioral measurements from each fly and flies dispersed for many meters along stable (or very slowly changing) angles relative to the bar, the flies were likely using the visual stimulus as a landmark to help them maintain a stable orientation. Formally, however, it remained possible that flies were largely ignoring the visual stimulus and maintaining stable trajectories via proprioceptive feedback from their legs, for example. We therefore measured the orientation behavior of the same flies in complete darkness and found that they did not walk nearly as straight over 60 s windows (data points near the center of the polar plot, Supplementary Figure 1b-d), even though their first-order walking statistics over shorter timescales were quite similar in the dark and with the bar (Supplementary Figure 1e). Thus, visual feedback is necessary for flies to stably maintain their direction. Beyond 60 s, flies often continued to maintain a consistent heading relative to the bright bar for many minutes (Supplementary Figure 1d, top), but were not able to do so in the dark (Supplementary Figure 1d, bottom).

Previous studies have noted that flies orient directly toward (*front-fixation*) or away (*anti-fixation*) from simple visual stimuli¹⁷⁻²². The behavior we observed, which we call *arbitrary-angle fixation*, is different in that flies stabilize a stimulus at seemingly arbitrary angles relative to their body axis. In control experiments, we found that tethered, walking *Drosophila* indeed tend to front-fixate or rear(anti)-fixate vertical *dark* bars, but they maintain bright bars—the principal stimulus used in this paper—at stable, but arbitrarily chosen angles relative to their body axis (Supplementary Figure 2). Orienting directly toward or away from a dark bar is consistent with the flies interpreting the dark stimulus as an object to either approach or avoid. Arbitrary-angle fixation of bright bars in walking flies (Figure 1) instead resembles previous reports of tethered, flying flies maintaining an arbitrary heading relative to certain visual stimuli (i.e., *menotaxis*)^{9,10} or to the angle of polarized light^{23,24} and is most readily interpreted as an attempt by the flies to disperse along a specific, but randomly chosen, bearing for a long distance, with the bright bar serving as a distant beacon to help maintain a straight trajectory. While more work will be required to fully delineate the conditions that promote front/anti-fixation vs. arbitrary-angle fixation, all genotypes we studied reliably performed arbitrary-angle fixation with bright bars, even while imaging neural activity, allowing us to examine how this behavior is implemented at the neural level.

Flies maintain a goal heading

The dark experiments demonstrate that visual feedback is generally important for observing effective long-range dispersal, but how do flies use the bar to walk straight? One possibility is that flies stabilized only the left/right movements of the bar, while ignoring its angular position. Alternatively, the flies might have maintained a specific angular bearing relative to the landmark. To distinguish between these options, we measured the flies' behavioral responses to abrupt, experimentally-introduced rotations in the visual scene (i.e., the blue bar) (Figure 2). Specifically, we discontinuously rotated (or “jumped”) the bar $\pm 90^\circ$ or 180° relative to its current angular position while flies were performing arbitrary angle fixation (Figure 2a). We analyzed the ~90% of trials where the flies' headings were relatively constant (circular s.d. $< 45^\circ$) before this experimental perturbation, since this criterion made it more likely that the flies were attempting to walk straight at the moment we jumped the bar. We found that following bar jumps, flies typically turned on the ball so as to return the bar to the angular position it occupied before the jump (Figure 2b-c, Supplementary Figure 3a-b, Video 1, 2). Flies could compensate for bar rotations starting from any angular position in the arena (Supplementary Figure 3a,c-d). On trials where they did not return the bar, the flies tended to walk more slowly, suggesting that on these trials the flies were not as engaged or may have needed more time to return the bar (Supplementary Figure 3e-f). Flies returned the bar to its previous angle even after 30 s of darkness (Supplementary Figure 3g), indicating that they remembered the bar's initial angular position for at least 30 s. That flies return the bar to its initial angle after 180° rotations and after 30 s of darkness negates the idea that the flies were only stabilizing the bar's angular velocity. Rather, the flies were clearly maintaining a specific angular bearing relative to the bar, which we call the fly's *behavioral goal angle*.

To return the bar to the behavioral goal angle after a bar jump, flies turned left when the bar was on the left and turned right when the bar was on the right (Figure 2d-e). We also observed that flies reduced their forward walking velocity after bar jumps (Figure 2f-g), consistent with the interpretation that the flies aim to walk forward fast only when the bar is in the desired, or goal, position. The fact that flies slowed down their forward speed after 180° bar jumps even on the subset of trials when, immediately after the jump, the flies turned relatively little (Supplementary Figure 4) argues that slowing down reflects a separable behavioral response from turning. Moreover, we observed that both the flies' turning and forward velocities were quantitatively modulated as a function of distance to the behavioral goal angle (Figure 3). (Although we jumped the bar $\pm 90^\circ$ or 180° , we analyzed turning strength throughout the return trajectory, with the bar positioned at various intermediate angles relative to the initial angle.) Thus, two distinct actions, turning and slowing down, appear tied to the difference between the fly's current heading and behavioral goal heading in this task.

E-PG activity tracks current heading, not goal heading

How might signals in the brain allow flies to perform arbitrary-angle fixation? Recent work has identified several neuron classes in the fly central complex (Figure 4a) that carry heading signals. For example, ellipsoid body-protocerebral bridge-gall neurons²⁵ (or *E-PGs* for short) show a single calcium activity peak, or bolus, that rotates around the donut-shaped ellipsoid body⁶, and 2–3 boluses that move left and right across the linear protocerebral bridge^{14,26}, with the position of these peaks correlating with the fly's virtual heading^{6,14,26}. To date, studies have focused on understanding how E-PG activity is built²⁷ or updated when the fly turns^{6,14,26}; how E-PG activity (or head-direction cell activity in any species) guides moment-to-moment behavior remains unknown.

Although previous studies have shown a strong correlation between the position of the E-PG boluses in the ellipsoid-body/bridge and the fly's angular heading, these experiments could not formally distinguish between the possibility that E-PG activity carries a straightforward current-heading signal from the possibility that E-PGs instead carry a goal-heading or a goal-minus-current-heading signal. In principle, each small rotation of the E-PG boluses might have represented a small change in the fly's *desired* heading, or the fly's current heading relative to a desired heading angle, rather than a simple update of the fly's best estimate of its current heading in the world, independent of any behavioral intention it may have had at the moment. To distinguish among these options, we reasoned that during experimental rotations of the bar (i.e., "bar jumps"), a goal signal would stay unchanged in the brain since the fly reacts to this perturbation by turning so as to bring the rotated bar back to its original position (Figure 2), arguing that the goal position was not altered by the bar jump on most trials. A heading signal, on the other hand, should update with the bar's new location on the arena since the repositioned visual cue provides evidence to the fly that its heading has changed (Figure 4b). We imaged E-PG activity in the protocerebral bridge under two-photon excitation¹²⁻¹⁴ with GCaMP6f²⁸ while flies performed arbitrary-angle fixation (Figure 4c). When we performed bar jumps, we found that the position, or *phase*, of the periodic E-PG calcium boluses in the bridge (i.e. the *E-PG phase*) consistently updated with the repositioned bar (Figure 4c-d), which is inconsistent with the E-PG phase

representing the fly's goal (Figure 4b). These results recapitulate those previously reported in bar-jump experiments with E-PGs⁶, but since flies in past experiments were not performing any clear task—and thus no goal direction was defined—one could not formally differentiate between the E-PG phase reflecting current heading versus goal heading. Another possibility we ruled out is that the E-PG phase tracks the fly's heading *relative* to the goal (like the neurons reported in Sarel et al.⁷). We imaged E-PG activity in flies that exhibited two or more stable goal directions during a single imaging session and found that the E-PG phase consistently followed the position of the bar on the arena, independent of the goal direction, as expected from a straightforward heading signal that is ignorant of the fly's behavioral intention during arbitrary-angle fixation (Supplementary Figure 5).

Impairing E-PG physiology impairs goal-directed navigation

If, as shown above, the E-PG phase tracks the fly's current heading independent of the goal heading during arbitrary-angle fixation, one may wonder whether E-PGs serve any role at all in guiding goal-directed behavior. We therefore inhibited synaptic output from a broad set of E-PGs (potentially all of them), and asked whether flies could still perform arbitrary angle fixation. We expressed in E-PG neurons *shibire^{ts}*, a dominant mutant of dynamin that impairs synaptic transmission at high temperatures (> 29°C)²⁹. Naïvely, one might not expect a neuron's calcium signals to be impacted by blocking its own synaptic outputs, but past work has argued that E-PGs participate in a recurrent circuit that helps to maintain their own activity^{6,14,25-27}, in which case, inhibiting E-PG synaptic output should impair E-PG physiology. Indeed, although E-PG neurons remained active when E-PG synaptic release was inhibited at 34°C, the E-PG phase was highly unstable, and poorly tracked the fly's heading, both with a closed-loop bar (Supplementary Figure 6a-d) and in the dark (Supplementary Figure 6e). (We note that the E-PG phase *velocity* tracked the bar *velocity* reasonably well even in E-PG>*shibire^{ts}* flies, but not well enough to prevent the heading signal from drifting wildly, see Supplementary Figure 6d.)

We measured the effect of impairing E-PG synaptic output on the flies' walking behavior (Figure 5). As one would expect from impairing a heading signal, E-PG-impaired flies were worse at maintaining a consistent heading in closed-loop with a bar (Figure 5), did not disperse as far as controls (Supplementary Figure 7), and were poor at correcting for rotations in the visual scene (Supplementary Figure 8). Intriguingly, further analysis of both our closed-loop walking (Figure 5d) and bar jump (Supplementary Figure 8) experiments revealed that E-PG-impaired flies retained a residual ability to maintain the bar in front, albeit with more angular variance than the arbitrary-angle fixation seen in control flies (i.e. data points closer to the center in Figure 5d). This residual frontward bias may rely on visual-motion sensitive neurons³⁰ or visual-object sensitive neurons³¹⁻³⁴, whose signals can perhaps bypass E-PGs to impact the leg motor system. Thus, E-PG-impaired flies show a residual form of front-bar fixation, but cannot effectively maintain their heading at an arbitrary angle relative to a visual landmark for extended periods.

E-PG-impaired flies turned weakly in response to bar jumps (Supplementary Figure 9). We note, however, that E-PG-impaired flies also generally walked slower than control flies (Supplementary Figure 9c). Controlling for this slower baseline forward walking speed (i.e.

selecting for trials where control flies walked at similar forward speeds as E-PG-impaired flies) appears to largely account for the reduced turning response in E-PG-impaired flies (Supplementary Figure 9d-e). Thus, the weak turning responses may, at least in part, be due to an indirect effect from the slow forward walking speeds of *shibire^{ts}*-affected flies. (Because E-PG>*shibire^{ts}* flies can maintain, albeit not so stably, the bar in front, we also expect some residual ability to correct for bar jumps.) On the other hand, E-PG-impaired flies showed no obvious decrease in forward walking speed following bar rotations (Supplementary Figure 9c,i), even after controlling for baseline walking speeds of *shibire^{ts}*-affected flies (Supplementary Figure 9f-g).

Overall, despite the abovementioned caveats, E-PG impaired flies were not able to stably maintain a bar on the side or in the rear, demonstrating a fundamental impairment in their ability to perform arbitrary-angle fixation. These behavioral effects were consistent across all three E-PG-expressing Gal4 lines (Figure 5, Supplementary Figure 6-9). Anatomical evidence argues that the only cells consistently inhibited across the three Gal4 lines are E-PGs (Figure 5c, Supplementary Figure 10 and Supplemental Table 1).

Chemogenetically rotating the E-PG heading signal induces corrective turns

The E-PG silencing experiments argue for a general role of E-PG synaptic output in allowing flies to perform arbitrary angle fixation, but do not distinguish among models for *how* the E-PG heading signal guides oriented navigation. We therefore performed neural stimulation experiments that redirected the fly's E-PG boluses to a new angle within the ring-like heading circuit (Figure 6). We considered three possible outcomes for this experiment. (1) If flies aim to maintain their E-PG boluses at a goal angle, the flies should turn in a direction that would bring their E-PG heading signal back toward the angle it occupied prior to stimulation (Figure 6a, left). (2) E-PG rotations might always directly drive the fly's turning behavior, like a steering wheel; in this case, the flies should turn as they normally would for the same E-PG rotation without stimulation, and in the opposite direction predicted by outcome 1 (Figure 6a, middle). (3) If flies walk forward independently of the exact position of the E-PGs, the flies should not turn with directionality (that is, not turn at all, or respond in a complex manner) in response to this perturbation (Figure 6a, right). Past work in which the fly's heading signal was rotated did not focus on behavior, reporting only in passing either anecdotal turning¹⁴ or gross increases in the rate of turns²⁷.

We experimentally rotated the E-PG phase by activating P-ENs (protocerebral bridge-ellipsoid body-noduli)²⁵, cells that are known to excite E-PGs^{14,26}. (See Methods for why we did not stimulate E-PGs directly.) We expressed in P-ENs the ATP-gated cation channel P2X₂, and locally released ATP on 1–2 glomeruli in the bridge (Figure 6a-c). This stimulation repositions the E-PG phase in the bridge by both activating E-PGs just medial to the stimulated location and by suppressing E-PGs (via as-of-yet uncharacterized circuitry) where they were originally active^{14,27}. We measured the effect of this stimulation both on E-PG activity with GCaMP6f, and on the fly's behavior. We performed these experiments in complete darkness, to avoid providing conflicting inputs to the system because any visual cue would not have rotated in sync with our neural stimulation. Although flies do not

maintain a consistent virtual heading on the ball in darkness (Supplementary Figure 1b-d), we observed that flies walking in the dark do maintain their *E-PG phase* in nearly as stable a position in the brain as when they walked with a closed-loop bar (Supplementary Figure 11), suggesting, remarkably, that flies walking in darkness may be actively attempting to maintain a straight trajectory with respect to their E-PG heading signal, even if their actual trajectories on the ball drift due to lack of visual feedback. (The E-PG heading signal is known to rapidly drift relative to the fly's behavioral heading on a ball in the dark^{6,14}).

After experimentally rotating the E-PG boluses, we observed that flies turned on the ball in a manner that was consistent with the first outcome in Figure 6a (data in Figure 6d-g). That is, they turned in a direction that would act to bring the E-PG boluses back to the positions they occupied in the protocerebral bridge prior to stimulation (Video 3, 4). The side of the bridge in which we stimulated (left vs. right) could not explain the direction in which the flies turned (Supplementary Figure 12a), and we observed no consistent behavioral turns in flies lacking a Gal4 transgene (Supplementary Figure 12b), arguing that these behavioral responses were caused by the rotation of the E-PG/P-EN phases (which are yoked to each other^{14,26}), specifically. We also observed a decrease in forward velocity upon stimulation, which depended on the angular distance between stimulated and initial E-PG phases (Figure 6h-i). Moreover, both the flies' turning and forward walking responses were quantitatively tuned to the position of the E-PG phase relative to its pre-stimulation position (Figure 7). Notably, the behavioral consequences of chemogenetically rotating the E-PG heading estimate in the dark mirrored those of experimentally rotating the visual scene (Figure 2), supporting the hypothesis that a similar underlying E-PG phase-dependent computation underlies these two behaviors.

Discussion

Previous work on the circuit anatomy^{25,35} and physiology of the central complex has highlighted its role in building²⁷ an internal estimate of angular heading⁶, whose value can be updated based on the fly's angular velocity^{14,26} and the position of visual landmarks^{34,36} (reviewed here^{37,38}). Other work has highlighted the role of the central complex in general locomotor control³⁹ as well as in the regulation of more sophisticated navigational tasks, such as oriented navigation^{9,40,41} and place learning⁴² (reviewed here³⁸). Our work here begins to bridge these two lines of research by characterizing how a central complex heading signal influences moment-to-moment actions during goal-directed navigation.

A limitation of the current study is that we do not explicitly identify a neural substrate for the fly's goal heading angle, but only infer its existence from other behavioral and neural measurements. As such, explicit models for how the goal-directed behavior we describe is implemented by the fly brain must remain necessarily speculative. Figure 8 presents two high-level, tentative models for how this computation could be performed, whose validity should be evaluated in future work.

One possibility is that the fly pattern-matches visual features on its retina to a reference or "goal" visual pattern⁴³, allowing it to walk at a consistent angle relative to the bright bar (Figure 8a). This model is generally consistent with the behaviors observed in Figures 1-3—

where a visual stimulus was present—but it would not account for the neural stimulation results in Figures 6-7, which were performed in darkness. It is possible that the fly uses an entirely different (non-visual-pattern-matching) mechanism that relies on E-PG neurons in the dark. However, the fact that normal E-PG activity is also required for flies to keep to a straight heading with visual feedback (Figure 5) argues against this interpretation. Moreover, that the flies' behavior in response to a rotation of the visual scene mirrors their response to a chemogenetically-induced rotation of their E-PG heading signal in the dark suggests that a common computation may underlie the flies' behavior in the dark and with a closed-loop bar.

A second model (Figure 8b) is that the E-PG phase tracks the fly's current heading, and a different set of neurons or synapses, not yet identified, store a goal heading, whose value is stable for minutes at a time. In this model, the fly brain quantitatively compares its estimate of current heading (in E-PGs) with the goal heading representation and uses this difference to control which way to turn and how hard to turn. If the E-PG phase is positioned counterclockwise relative to the goal (when viewing the ellipsoid body from the rear), the fly tends to turn left, which is the direction that causes its E-PG phase to rotate clockwise, back towards the internal goal heading. Conversely, if the E-PG phase is positioned clockwise relative to the goal, the fly tends to turn right. If the E-PG phase is aligned with the goal heading, flies speed up, enabling them to disperse far along the goal direction. This closed-loop system would allow flies to maintain a steady heading, as estimated by their E-PG phase, for hundreds of body lengths. One possibility is that this second model explains the flies' behavior in the dark, but is aided by visual-pattern-matching when visual feedback is present. An important variant of this second model worth considering is that the fly might compare an internal estimate of its current 2D position (e.g. a vector in relation to a start position) with a goal 2D position (a second vector), in which case the effects that we observe here may represent an initial, purely angular, window into what is an inherently vectorial computation.

Previous work in bats has identified neurons whose activity is quantitatively tuned to the angle of a landing platform (to which the bats are trained to land) relative to the angle at which the bat's head is pointed⁷ (analogous to the "error" signal in Figure 8b), suggesting that a comparison between current- and goal-heading guides the bat's navigational actions. Our work hints at a similar framework for goal-directed navigation in the fly via a different line of experiments (see second model above). Identifying the nature and biological locus of the fly's internal goal will help flesh out how the navigational behavior presented here is implemented at the circuit level. More generally, our work demonstrates that measuring the behavioral consequences of coherently manipulating an entire population of neurons carrying a cognitive signal can provide a useful experimental counterpart to correlating the same unperturbed signal with behavior, in terms of gaining insight into the roles of cognitive signals in guiding actions.

Methods

Fly stocks.

Flies were raised with a 12 hour light, 12 hour dark cycle. All experiments on plate tethered flies were performed with 1–3 day old females with at least one wild-type white allele. Experiments with pin-tethered flies were performed on slightly older females (3–6 days old). Flies were selected randomly for all experiments. We excluded flies that appeared unhealthy at the time of the experiment. We were not blind to the flies' genotypes. Genotypes and their origins are listed in Supplemental Tables 2, 3.

Immunohistochemistry.

Dissection of fly brains, fixation, and staining for neuropil and multicolor flip-out antigens were performed as previously described^{14,46}.

Plate-tethered behavioral setup.

Tethered walking, behavioral imaging, ball tracking, and closed-loop visual feedback were setup as previously described¹⁴. We used different rigs for behavioral and imaging experiments that both made use of the plate-tether. For the behavioral rig, we recorded data on a National Instruments BNC-2090A A/D converter. For the imaging rig, we recorded data on an Axon Instruments Digidata 1440 A/D converter. Otherwise the two rigs were as identical as possible, including matching the fly's position relative to the LED display (arena) and the angle of the LED display (see Behavioral task below). We recorded behavioral data at 50 Hz. The temperature of the fly's head and upper thorax were controlled by the temperature of water (or physiological saline in the case of imaging experiments) flowing over these body regions.

Plate-tethered behavioral conditions.

Flies were food deprived for 8–16 hours prior to testing, and were heated via the water or saline bath to at least 30°C (measured in the bath), except for E-PG>*shibire^{ds}* control imaging experiments, where we kept the bath at 26°C (Supplementary Figure 6). We originally used these conditions to simply promote walking; however, we also found that the flies tended to maintain their heading at a consistent, but arbitrary angle with respect to the bar under these conditions. We note that these experimental parameters likely reflect an uncomfortable situation for the fly, and that the fly is likely reacting by attempting to disperse, or search a large area in search of food or cooler temperatures. The flies' heads were glued to our fly plates with a downward pitch (antennae angled down, toward the ball), since this posture facilitated protocerebral bridge imaging and ATP stimulation with a pipette. We kept this posture consistent across all imaging and plate-tethered behavioral experiments, like in the original studies that developed this preparation¹³. To partially account for this pitch, we tilted the arena 30° forward with respect to the horizontal (angled arena in Figure 1a), to better match the angle of the fly's head. However, it is likely that the flies still viewed the bright bar with their dorsal visual field, which might lead them to interpret our bright visual landmark (see below) as a celestial cue, useful for orienting their dispersal.

Plate-tethered visual stimuli.

We used a cylindrical LED arena¹⁵, spanning 270° in azimuth, and 81° in height. However, we note that the ball below the fly and the physiology plate above the fly's head acted as visual occluders, allowing the flies to see only ~45–50° of the full height of the bar. For closed-loop bar experiments, we presented the fly with a 6 pixel-wide (11.25°), 81° high bright bar. The bar rotated with the ball with a gain of 1. For discontinuous rotations of the visual stimulus, the fly was presented with a closed-loop bar, except for one frame every trial where the bar jumped –90°, +90° or 180° from its current position. Immediately after the bar jump, it resumed rotating in closed-loop with the fly from its new position. For the 30 s dark stimulus, the fly was presented with a closed-loop bar for 3 minutes, then 30 s of constant darkness, after which the bar reappeared with a random offset with respect to the ball. For all experiments with a closed-loop bar, we let the fly walk in closed-loop with the bar for at least 5 minutes before beginning each experiment. Trial orders were randomly permuted for all experiments. See Supplemental Table 2 for trial structure for each experiment.

Pin-tethered experiments.

For Supplementary Figure 2, we tethered 3–6 day old Canton-S flies to rigid (tungsten) pins rather than plates, to ensure that no plastic from the physiology plate impeded their field of view, and to be able to test many parameters effectively (pin-tethering takes less time). In these experiments, we used a cylindrical LED display spanning 330° in azimuth and 105° in height. We used a standard, green (570 nm) LED display, with 3.75° azimuthal pixel resolution; because the *Drosophila* visual system has ~5° spatial resolution, 3.75° per pixel is sufficient for many behavioral tests. We used 4-pixel (15°) wide, 105° high bright or dark bars. Because pin-tethered flies (unlike plate-tethered flies) had no temperature-controlled saline bath flowing over them, we heated flies with a thermal IR laser (980 nm) aimed at the back of the head and thorax to motivate walking. We increased the intensity of the laser (via pulse-width modulation) until the fly began walking robustly. We did not measure the temperature of the flies in these experiments. Preliminarily, we noticed that both plate- and pin-tethered flies tended to keep a dark stripe directly behind them (anti-fixation), which was at odds with a past report that argued for robust front fixation of tall dark stripes¹⁷. To examine this discrepancy with past work, we manipulated many parameters in pin-tethered flies to determine if any specific one might have a large effect on the flies' propensity to orient directly toward the dark bar (e.g., fly age, fly strain, time of day, stimulus height, stimulus contrast, closed-loop gain, intensity of dark spots on the ball used by Fictrac for tracking, location of heat laser on the fly's body, etc.). We found that when we raised the air flow rate on the air-cushioned ball—to a level where we just started to see the fly's wings flutter and the ball start to jitter from the more turbulent air flow—the flies began to spend more time (~50%) orienting directly toward the dark bar (fixation) than in other conditions, in which they front-fixated rarely. (High air flow from below was also provided in a previous report of front-fixation¹⁷, and did not impede the flies from walking forward robustly and quickly in our setup.) On the other hand, pin-tethered flies performed arbitrary-angle fixation in reference to bright objects, both with low air flow (Supplementary Figure 2d) and high air flow (data not shown). Flies were not food deprived prior to being pin-tethered, though they did remain on the tether, without food, for ~1–8 hours before being tested.

Imaging setup.

Calcium imaging, two photon data acquisition and alignment with behavioral data were performed as previously described¹⁴. We excited GCaMP6f with a Chameleon Ultra II Ti:Sapphire tuned to 925 nm, with 20–50 mW at the back aperture. We recorded all imaging data using 3–6 z-slices at a volumetric rate of 4–6 Hz. In all figures, the left protocerebral bridge is shown on the left, and the right bridge on the right. In Video 3, 4, this orientation is flipped, since the fly is viewed from the front. We perfused the brain with extracellular saline composed of, in mM: 103 NaCl, 3 KCl, 5 N-Tris(hydroxymethyl) methyl-2-aminoethanesulfonic acid (TES), 10 trehalose, 10 glucose, 2 sucrose, 26 NaHCO₃, 1 NaH₂PO₄, 1.5 CaCl₂, 4 MgCl₂, and bubbled with 95% O₂ / 5% CO₂. The saline had a pH of 7.3–7.4, and an osmolarity of 280±5 mOsm.

P2X₂-based stimulation.

The most straightforward way to reposition the phase of the E-PG signal in the protocerebral bridge would be to stimulate E-PGs directly. Although we could reliably stimulate E-PGs by expressing P2X₂ in them directly (data not shown), we were not able to induce bilateral changes in E-PG activity in the bridge by stimulating a single location on one side of the bridge with stimulation strengths that elicited E-PG responses within their physiological range. However, we could regularly achieve a naturalistic, bilateral, re-positioning of the E-PG activity peaks via stimulation of a different cell class in the central complex, called P-ENs, at one location in the bridge (Figure 6). P-EN neurons from one glomerulus on one side of the bridge project to a tile in the ellipsoid body that contains E-PG neurons that project to the left bridge as well as E-PG neurons that project to the right bridge²⁵, which may explain why P-EN stimulation in the bridge is more effective at repositioning E-PG activity bilaterally. We note that others were able to relocate the E-PG activity peak by directly activating E-PGs via optogenetic stimulation in the ellipsoid body²⁷, which is innervated by E-PGs from both sides of the bridge. We preferred to chemogenetically activate E-PGs (via P-ENs), since we found that optogenetic light stimulation tended to cause the fly's behavior to change (including turning), irrespective of whether we expressed a light-activated channel in the brain. Thus, we stimulated E-PGs by chemogenetically exciting P-ENs. Specifically, we expressed in P-ENs the ATP-gated cation channel P2X₂, and focally released ATP from a pipette via pressure pulses, as described previously¹⁴. Unlike previous experiments, however, here we analyzed the fly's behavioral responses to stimulations and provided ATP pulses with longer inter-pulse intervals (2 min.) to ensure that flies had ample time to behaviorally correct for each perturbation. We used 0.5 mM ATP in extracellular saline delivered with 20–50 ms pressure pulses. To compute the stimulated E-PG phase, we computed the mean E-PG phase over 0.5 to 1 s after stimulations for each recording. We collected data from 17 experimental and 15 control flies.

Data analysis.

Two photon images over time were first registered along the x-y plane using python 2.7, as described previously¹⁴. Regions of interest highlighting the 18 glomeruli in the bridge were then manually parsed in Fiji^{14,47} and all subsequent analyses of these signals were performed in python 2.7 as described previously¹⁴. Some flies, which seemed excessively

food deprived and appeared quite unhealthy as a result, were not analyzed. With pin-tethered flies, since we were not measuring the flies' temperature, some flies died from excessive laser-based heating during the experiment, and these were excluded. Otherwise, no flies were excluded. No statistical method was used to choose the sample size. When plotting turning or forward velocity over time (e.g. Figure 2, Figure 6), these signals were smoothed with a 200 ms Gaussian filter.

Computation of mean heading vectors.

We treated each heading measurement as a unit vector, and computed the mean of these heading vectors over a given window length of the fly walking (e.g. 60 s in Figure 1d). To ensure that we did not artificially overestimate the propensity of flies to perform arbitrary-angle fixation, heading measurements associated with time points in the analysis window where the fly was standing still (forward velocity < 0.5 mm/s) were omitted from contributing to the mean heading vector calculated in that window because when the fly stands still, its heading is constant at an arbitrary angle for trivial reasons. We slid the analysis window over the heading time series within each trial (e.g. 60 s in Figure 1), by 1 s increments, and calculated the mean-heading vector at each position, ultimately plotting the distribution of all mean heading vectors for a given trial type in a 2-dimensional polar histogram. Data near the edge of the circle of such a histogram indicate walking along a consistent bearing whereas data near the middle indicate many changes in heading over the analyzed time window¹⁸. We additionally calculated the mean vector length in each polar plot and then plotted the distribution of mean heading vector magnitudes of polar plots generated with analysis windows of different time durations (Supplementary Figure 1, 7, 11). Such a plot acts as a measure of how well flies maintain their heading over different timescales because if the mean vector of polar plots remains high with, for example, 400 s analysis windows, this indicates that flies must be maintaining consistent walking angles over 6+ minutes.

Computing turning and forward walking as a function of distance to the initial heading.

Analyzing data from before and after bar jumps (-20 to 40 s), we computed 2D histograms of turning or forward walking velocity, as a function of distance to the initial heading (Figure 3, Figure 7, Supplementary Figure 9). Like in all plots analyzing bar jump data, we defined the fly's initial heading as the mean heading 10 s before bar jumps. We also computed the mean turning signal as a function of distance to the initial heading (black trace). One can plot these data with different delays between the turning velocity signal and the distance to goal signal. In all figures, we plot the data using the delay between the motor signal (e.g. turning or forward velocity) and the distance to goal signal at which the fly turned strongest as a function of distance to goal. This optimal delay was 350 ms for Figure 3 and Supplementary Figure 9, and is consistent with the idea that the fly first processes information about the position of the bar, as well as other sensory and internal inputs, to compute its heading, and then translates this heading signal through further processing (for example, via the model in Figure 8) into a turning command. For Figure 7, we found that the turning response was strongest at 100 ms after the distance-to-goal E-PG phase signal, consistent with the E-PG phase signal (which is derived from the fly's internal heading estimate) being closer in time to the fly's motor command to turn than is a visual stimulus.

We used 300 ms-Gaussian-filtered turning and forward walking signals for these analyses to smooth the turning and forward walking signals. The delays reported here are therefore expected to be approximate.

Statistics.

We used two-sided Wilcoxon signed-rank and rank-sum tests for paired and non-paired data, as indicated in the relevant figures. In all figures, 95% confidence intervals were computed by bootstrapping.

Code availability.

Code is available from the corresponding author upon request.

Life Sciences Reporting Summary.

Please see the Life Sciences Reporting Summary published alongside this article.

Data availability

The data that support the findings of this study are available from the corresponding author upon request.

Supplementary Material

Refer to Web version on PubMed Central for supplementary material.

Acknowledgements

We thank the laboratories of V. Ruta (The Rockefeller University) and G. Rubin (Janelia Research Campus) for fly stocks, L. Fenk, S. Jereb and D. Wilson for comments on the manuscript, and members of the Maimon laboratory for helpful discussions. Stocks obtained from the Bloomington Drosophila Stock Center (NIH P40OD018537) were used in this study. This work was supported by the McKnight Foundation (G.M.), the National Institutes of Health (DP2DA035148 and R01NS104934) (G.M.) and the Leon Levy Foundation (V.V.). G.M. is a Howard Hughes Medical Institute Investigator.

References

1. Tsoar A et al. Large-scale navigational map in a mammal. *PNAS* 108, E718–24 (2011). [PubMed: 21844350]
2. Müller M & Wehner R Path integration in desert ants, *Cataglyphis fortis*. *PNAS* 85, 5287–5290 (1988). [PubMed: 16593958]
3. Taube JS, Muller RU & Ranck JB Head-direction cells recorded from the postsubiculum in freely moving rats. I. Description and quantitative analysis. *J. Neurosci.* 10, 420–435 (1990). [PubMed: 2303851]
4. Heinze S & Homberg U Maplike Representation of Celestial E-Vector Orientations in the Brain of an Insect. *Science* 315, 995–997 (2007). [PubMed: 17303756]
5. Varga AG & Ritzmann RE Cellular Basis of Head Direction and Contextual Cues in the Insect Brain. *Current Biology* 26, 1816–1828 (2016). [PubMed: 27397888]
6. Seelig JD & Jayaraman V Neural dynamics for landmark orientation and angular path integration. *Nature* 521, 186–191 (2015). [PubMed: 25971509]
7. Sarel A, Finkelstein A, Las L & Ulanovsky N Vectorial representation of spatial goals in the hippocampus of bats. *Science* 355, 176–180 (2017). [PubMed: 28082589]

8. Butler WN, Smith KS, van der Meer MAA & Taube JS The Head-Direction Signal Plays a Functional Role as a Neural Compass during Navigation. *Current Biology* 27, 1259–1267 (2017). [PubMed: 28416119]
9. Giraldo YM et al. Sun Navigation Requires Compass Neurons in *Drosophila*. *Current Biology* 28, 2845–2852.e4 (2018). [PubMed: 30174187]
10. Heisenberg M & Wolf R in *Vision in Drosophila* 12, 146–157 (Springer, Berlin, Heidelberg, 1984).
11. Dacke M, Nilsson D-E, Scholtz CH, Byrne M & Warrant EJ Animal behaviour: insect orientation to polarized moonlight. *Nature* 424, 33–33 (2003).
12. Seelig JD et al. Two-photon calcium imaging from head-fixed *Drosophila* during optomotor walking behavior. *Nature Methods* 7, 535–540 (2010). [PubMed: 20526346]
13. Maimon G, Straw AD & Dickinson MH Active flight increases the gain of visual motion processing in *Drosophila*. *Nat Neurosci.* 13, 393–399 (2010). [PubMed: 20154683]
14. Green J et al. A neural circuit architecture for angular integration in *Drosophila*. *Nature* 546, 101–106 (2017). [PubMed: 28538731]
15. Reiser MB & Dickinson MH A modular display system for insect behavioral neuroscience. *J. Neurosci. Methods* 167, 127–139 (2008). [PubMed: 17854905]
16. Moore RJD et al. FicTrac: A visual method for tracking spherical motion and generating fictive animal paths. *J. Neurosci. Methods* 225, 106–119 (2014). [PubMed: 24491637]
17. Bahl A, Ammer G, Schilling T & Borst A Object tracking in motion-blind flies. *Nat Neurosci.* 16, 730–738 (2013). [PubMed: 23624513]
18. Maimon G, Straw AD & Dickinson MH A Simple Vision-Based Algorithm for Decision Making in Flying *Drosophila*. *Current Biology* 18, 464–470 (2008). [PubMed: 18342508]
19. Reichardt W & Poggio T Visual control of orientation behaviour in the fly. Part I. A quantitative analysis. *Quarterly reviews of biophysics* 9, 311–75 428–38 (1976). [PubMed: 790441]
20. Strauss R & Pichler J Persistence of orientation toward a temporarily invisible landmark in *Drosophila melanogaster*. *J. Comp. Physiol. A* 182, 411–423 (1998). [PubMed: 9530834]
21. Bülthoff H, Götz KG & Herre M Recurrent Inversion of Visual Orientation in the Walking Fly, *Drosophila melanogaster*. *J. Comp. Physiol.* 148, 471–481 (1982).
22. Horn E & Wehner R The mechanism of visual pattern fixation in the walking fly, *Drosophila melanogaster*. *J. Comp. Physiol.* 101, 39–56 (1975).
23. Weir PT & Dickinson MH Flying *Drosophila* Orient to Sky Polarization. *Current Biology* 22, 21–27 (2012). [PubMed: 22177905]
24. Warren TL, Weir PT & Dickinson MH Flying *Drosophila* maintain arbitrary but stable headings relative to the angle of polarized light. *J. Exp. Biol.* (2018). doi:10.1242/jeb.177550
25. Wolff T, Iyer NA & Rubin GM Neuroarchitecture and neuroanatomy of the *Drosophila* central complex: A GAL4-based dissection of protocerebral bridge neurons and circuits. *J. Comp. Neurol.* 523, 997–1037 (2015). [PubMed: 25380328]
26. Turner-Evans D et al. Angular velocity integration in a fly heading circuit. *eLife* 6, e23496 (2017). [PubMed: 28530551]
27. Kim SS, Rouault H, Druckmann S & Jayaraman V Ring attractor dynamics in the *Drosophila* central brain. *Science* 356, 849–853 (2017). [PubMed: 28473639]
28. Chen T-W et al. Ultrasensitive fluorescent proteins for imaging neuronal activity. *Nature* 499, 295–300 (2013). [PubMed: 23868258]
29. Poodry CA & Edgar L Reversible alteration in the neuromuscular junctions of *Drosophila melanogaster* bearing a temperature-sensitive mutation, *shibire*. *J. Cell Biol.* 81, 520–527 (1979). [PubMed: 110817]
30. Fenk LM, Poehlmann A & Straw AD Asymmetric Processing of Visual Motion for Simultaneous Object and Background Responses. *Current Biology* 24, 2913–2919 (2014). [PubMed: 25454785]
31. Kim AJ, Fitzgerald JK & Maimon G Cellular evidence for efference copy in *Drosophila* visuomotor processing. *Nat Neurosci.* 18, 1247–1255 (2015). [PubMed: 26237362]
32. Kele MF & Frye MA Object-Detecting Neurons in *Drosophila*. *Current Biology* 27, 680–687 (2017). [PubMed: 28190726]

33. Wu M et al. Visual projection neurons in the *Drosophila* lobula link feature detection to distinct behavioral programs. *eLife* 5, 7587 (2016).
34. Seelig JD & Jayaraman V Feature detection and orientation tuning in the *Drosophila* central complex. *Nature* 503, 262–266 (2013). [PubMed: 24107996]
35. Franconville R, Beron C & Jayaraman V Building a functional connectome of the *Drosophila* central complex. *Authorea* (2018). doi:10.22541/au.151537454.41878908
36. Sun Y et al. Neural signatures of dynamic stimulus selection in *Drosophila*. *Nat Neurosci.* 503, 262 (2017).
37. Green J & Maimon G Building a heading signal from anatomically defined neuron types in the *Drosophila* central complex. *Current Opinion in Neurobiology* 52, 156–164 (2018). [PubMed: 30029143]
38. Turner-Evans DB & Jayaraman V The insect central complex. *Current Biology* 26, R453–R457 (2016). [PubMed: 27269718]
39. Martin JP, Guo P, Mu L, Harley CM & Ritzmann RE Central-Complex Control of Movement in the Freely Walking Cockroach. *Current Biology* 25, 2795–2803 (2015). [PubMed: 26592340]
40. Neuser K, Triphan T, Mronz M, Poeck B & Strauss R Analysis of a spatial orientation memory in *Drosophila*. *Nature* 453, 1244–1247 (2008). [PubMed: 18509336]
41. Triphan T, Poeck B, Neuser K & Strauss R Visual Targeting of Motor Actions in Climbing *Drosophila*. *Current Biology* 20, 663–668 (2010). [PubMed: 20346674]
42. Ofstad TA, Zuker CS & Reiser MB Visual place learning in *Drosophila melanogaster*. *Nature* 474, 204–207 (2011). [PubMed: 21654803]
43. Wehner R, Michel B & Antonsen P Visual navigation in insects: coupling of egocentric and geocentric information. *J. Exp. Biol.* 199, 129–140 (1996). [PubMed: 9317483]
44. Manton JD et al. Combining genome-scale *Drosophila* 3D neuroanatomical data by bridging template brains. *bioRxiv* (2018). doi:10.1101/006353
45. Jenett A et al. A GAL4-Driver Line Resource for *Drosophila* Neurobiology. *Cell Reports* 2, 991–1001 (2012). [PubMed: 23063364]

Methods References

46. Nern A, Pfeiffer BD & Rubin GM Optimized tools for multicolor stochastic labeling reveal diverse stereotyped cell arrangements in the fly visual system. *PNAS* 112, E2967–E2976 (2015). [PubMed: 25964354]
47. Schindelin J et al. Fiji: an open-source platform for biological-image analysis. *Nature Methods* 9, 676–682 (2012). [PubMed: 22743772]

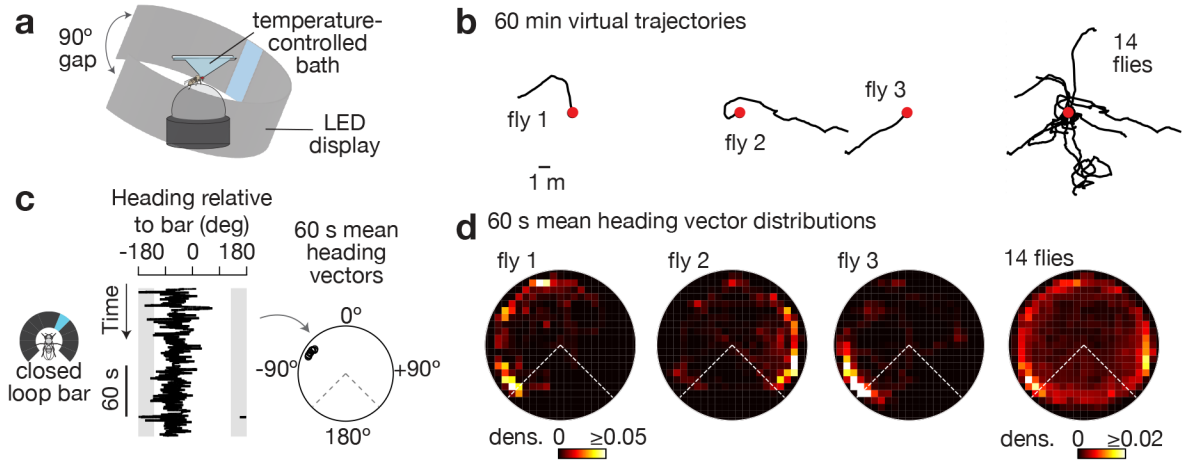


Figure 1. Tethered flies walk forward while maintaining a stable heading at an arbitrary angle relative to a visual landmark for minutes.

a, Tethered fly walking on a ball at the center of a 270° LED arena. **b**, 2D virtual trajectories of wild-type flies walking with a bright bar in closed-loop. Red dots indicate the starting point. Trajectories headed up on the page represent the flies walking towards the bar. **c**, Left: Heading relative to bar over 3 min for a sample fly. Right: We slid a 60 s analysis window over each heading trace and calculated the mean heading vector in each window (black circles, see Supplementary Figure 1 for Methods). **d**, Polar distributions of mean heading vectors taken over 60 s windows (slid by 1 s increments) for the flies shown above, in panel b. Time points in which flies were standing still (i.e. forward velocity < 0.5 mm/s) were ignored because heading values during such time points are stable for the trivial reason that the fly is not moving. Grey areas in c and dashed lines in d highlight the 90° gap of the LED display in which the bar is not visible.

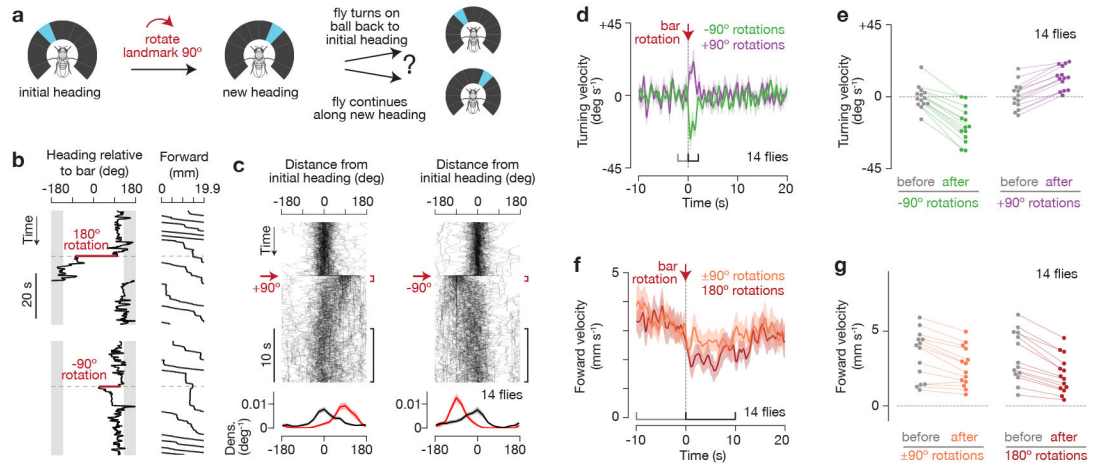


Figure 2. Flies actively maintain a stable heading relative to an angular goal.

a. As flies walked in closed-loop with the bar, we discontinuously rotated (or “jumped”) the bar $\pm 90^\circ$, and asked whether flies return the bar to its initial position. **b.** Heading relative to bar and forward walking during bar jumps. 19.9 mm of forward walking is equal to one rotation of the ball (360°). **c.** Top: Distance from initial heading over time for 90° bar jumps. The initial heading is defined as the mean heading in the 10 s window before the bar jump. In each panel, 90 traces from 14 flies are shown with 5% opacity. Bottom: Mean and s.e.m. of probability distributions of distance from initial heading at 0-1 s (red), and 10-20 s (black) after the bar jump. **d.** Mean and s.e.m. of turning velocity over time during 90° bar jumps. **e.** Mean turning velocity for each fly before (-2 to 0 s) and after (0 to 2 s) bar jumps (-90° : $p=0.002$, $+90^\circ$: $p=0.001$, two-sided Wilcoxon signed-rank test). **f.** Mean and s.e.m. of forward velocity over time during 90° and 180° bar jumps. **g.** Mean forward velocity for each fly before (-10 to 0 s) and after (0 to 10 s) bar jumps (90° : $p=0.004$, 180° : $p=0.001$, two-sided Wilcoxon signed-rank test). We analyzed the $\sim 90\%$ of trials where the flies maintained a relatively stable heading (circular s.d. $< 45^\circ$) for 10 s before the bar jump, as an indication that flies were performing arbitrary-angle fixation. No forward walking requirements were applied in this figure.

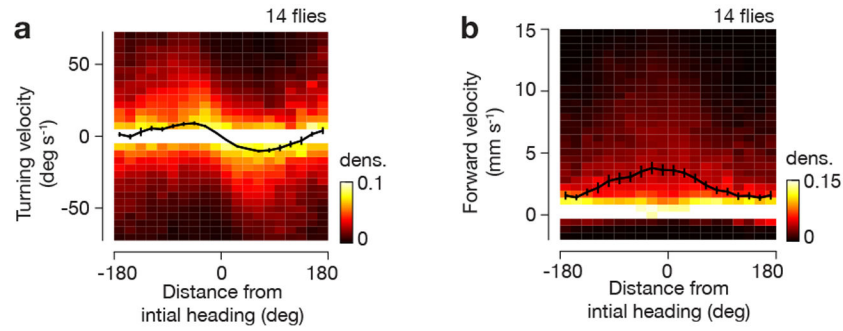


Figure 3. Flies quantitatively adjust their turning and forward velocity with respect to the angular distance of the bar from its initial position before a bar jump.

a. Turning velocity as a function of distance from initial heading during bar jumps, using data from -20 s to 40 s around bar jumps. Each column of the heat map is normalized independently (there are many more data points near $x=0$). Mean and s.e.m. across flies are shown (black curve). **b.** Same as **a**, but for forward velocity. For a-b, we only analyzed the $\sim 90\%$ of trials where the flies maintained a relatively stable heading (circular s.d. $< 45^\circ$) for 10 s before the bar jump, as an indication that flies were performing arbitrary-angle fixation.

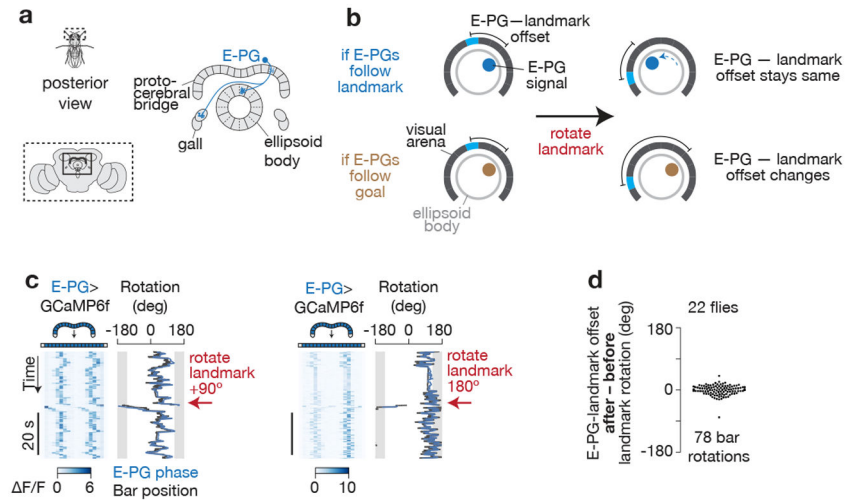


Figure 4. E-PG activity tracks the flies' heading and not their goal heading.

a, Posterior view of fly and central complex. The anatomy of a single E-PG neuron (blue). An array of E-PG neurons fully tile the ellipsoid body and almost fully tile the bridge²⁵. **b**, If the position of the E-PG boluses indicate the fly's heading, their position along the ring should consistently follow rotations of the bar; equivalently, the offset (or mean angular distance) between E-PG-bolus positions in the ring and the bar position on the LED screen should not change after bar jumps. If, on the other hand, the position of the E-PG boluses indicate the fly's goal heading, the offset between E-PG activity and bar position should change after bar jumps. **c**, E-PG activity during one 90° (left) and one 180° (right) bar jump, in two different flies. The 90° gap in the back of the LED display, where the bar is not visible, is highlighted in grey. To aid the visual comparison of the position of the E-PG boluses in the brain (the *E-PG phase*) and the bar position on the screen over time, we added a constant offset to the E-PG phase (blue) curve so as to minimize its distance from the bar position (black) curve, which is a standard transformation^{6,14} (see Methods). **d**, Change in offset after landmark rotations. That the changes in offsets are near zero indicates that E-PG activity tends to follow the rotation of the bar, and therefore that it tracks the fly's current heading and not the goal heading.

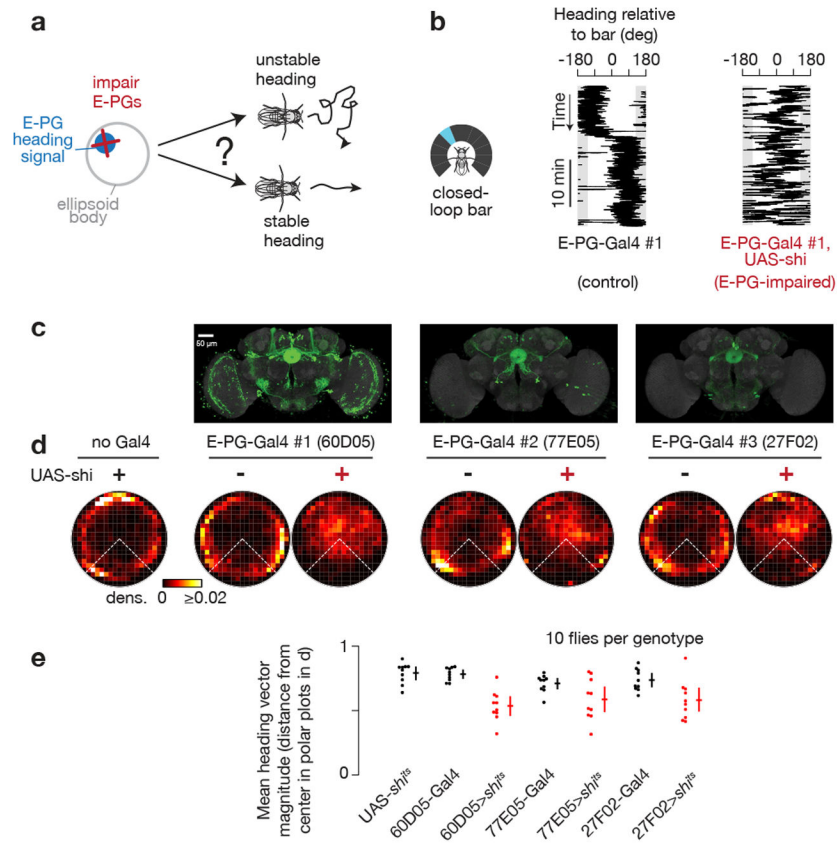


Figure 5. E-PG-impaired flies do not maintain a stable heading at an arbitrary angle.
a, Do flies maintain a stable heading when E-PG synaptic output is impaired? **b**, Heading of sample control and E-PG-impaired flies walking with a bar in closed-loop. **c**, Maximum z-projections of UAS-GFP expression in three different E-PG-expressing Gal4 lines (data from <http://www.virtualflybrain.org>^{44,45}, expression patterns confirmed by us). GFP expression is in green, neuropil in grey. **d**, Polar distributions of 60 s mean heading vectors (see Supplementary Figure 1 for Methods). **e**, Magnitude of 60 s mean heading vectors averaged for each fly (dots). Mean and 95% bootstrap confidence intervals across flies (crosses). Comparing UAS-*shi*^{ts} to X>*shi*^{ts}: $p=4e-4$ (60D05), $3e-3$ (77E05), $4e-3$ (27F02); comparing X-Gal4 to X>*shi*^{ts}: $p=5e-4$ (60D05), $8e-2$ (77E05), $1e-2$ (27F02), two-sided Wilcoxon rank-sum test. X> *shi*^{ts} indicates the combination of X-Gal4 and UAS- *shi*^{ts}. *shi*^{ts}-expressing flies are highlighted in red. Time points where the flies were standing still (i.e. forward velocity < 0.5 mm/s)—which yield stable headings, trivially—were ignored.

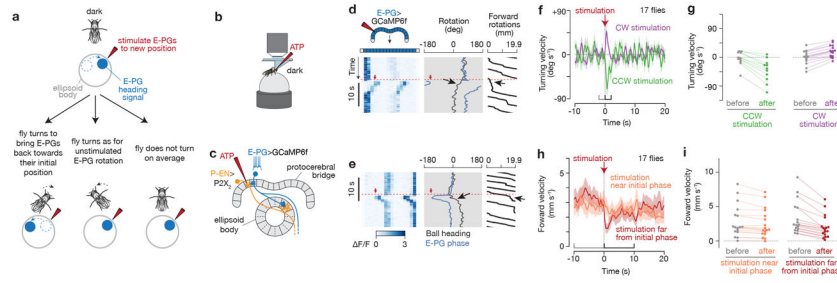


Figure 6. Flies slow down and turn to bring their E-PG activity back to its previous position in the protocerebral bridge after it is rotated via neural stimulation.

a. How does the fly react to a chemogenetically-stimulated change in its E-PG phase? See text for details on possible behavioral outcomes. **b-c.** We stimulated a different central-complex cell type, *P-ENs*^{14,25,26}, by expressing in them an ATP-gated ion channel ($P2X_2$) and puffing ATP with a pipette on specific glomeruli in the protocerebral bridge, while imaging E-PGs as flies walked in the dark. Stimulating P-ENs reliably repositions the E-PG phase medial to the stimulated P-EN glomerulus¹⁴ (Video 3, 4). **d-e.** E-PG activity (left), E-PG phase and fly heading (middle), and forward walking (right), during individual stimulation events. Red dashed lines mark stimulation time, red arrows mark stimulation position in the bridge. Black arrows highlight the fly turning and slowing down in response to stimulation. **f.** Mean and s.e.m. of turning velocity over time during events when our stimulation was positioned either clockwise or counterclockwise (45° to 135° away) relative to the initial E-PG phase. The initial E-PG phase is defined as the mean E-PG phase in the 10 s window before stimulations. **g.** Mean turning velocity for each fly before (-2 to 0 s) and after (0 to 2 s) stimulation (CCW: $p=3e-3$, 11 flies; CW: $p=2e-2$, 15 flies; two-sided Wilcoxon signed-rank test). The same flies were analyzed for both CCW and CW trials, only some flies by chance did not receive CCW or CW trials. **h.** Mean and s.e.m. of forward velocity over time when our stimulation was positioned either near ($<120^\circ$) or far ($>120^\circ$) from the initial E-PG phase. **i.** Mean forward velocity for each fly before (-10 to 0 s) and after (0 to 10 s) stimulation (near: $p=4.9e-2$, 17 flies; far: $p=3e-4$, 17 flies; two-sided Wilcoxon signed-rank test). We analyzed the 77% of trials where the E-PG phase was maintained at a relatively stable angle (circular s.d. $< 45^\circ$) for 10 s prior to ATP stimulation, as an indication that flies were performing arbitrary-angle fixation with respect to their E-PG phase. No forward walking requirements were applied to this figure. CW: clockwise. CCW: counterclockwise.

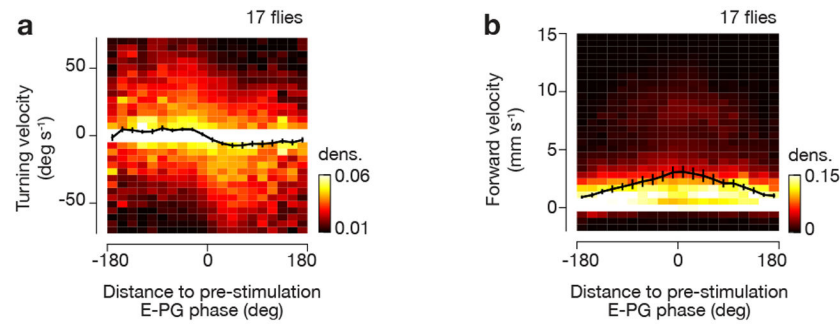


Figure 7. Flies walking in complete darkness quantitatively adjust their turning and forward velocities with respect to the angular distance between current E-PG phase and the E-PG phase prior to chemogenetic stimulation.

a, Turning velocity as a function of angular distance to the pre-stimulation E-PG phase using data from -20 s to 40 s around chemogenetic/ATP stimulation. **b**, Same as **a**, for forward velocity. Mean and s.e.m. across flies are shown (black curve). Note the slightly different scale of the heat map compared to Figure 3 and Supplementary Figure 9. We only analyzed the $\sim 77\%$ trials where the E-PG phase was maintained at a relatively stable angle (circular s.d. $< 45^\circ$) for 10 s prior to ATP stimulation, as an indication that flies were performing arbitrary-angle fixation with respect to their E-PG phase.

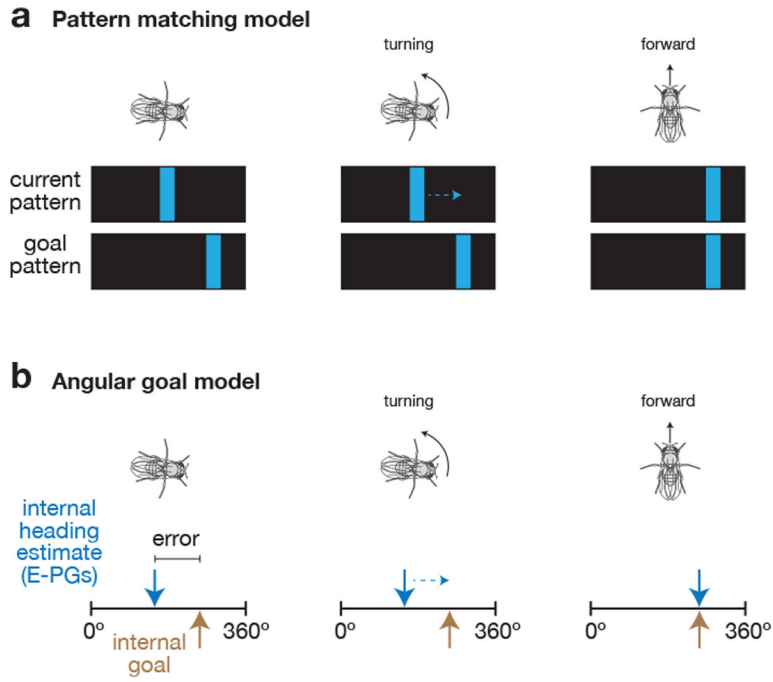


Figure 8. Working models for how flies perform goal-directed navigation.

a, Hypothesis that flies compare the pattern of visual features projected onto their retina with a goal feature pattern to guide navigational behavior. The fly turns to align the current pattern of visual features with the goal pattern in order to maintain its walking direction relative to its environment. **b**, Hypothesis that flies compare an internal heading estimate, carried by E-PGs, with an internal goal angle to guide navigational behavior. The fly turns to align its internal heading estimate (blue arrow) with an internal goal angle (gold arrow). When the two are aligned, the fly walks forward faster. See Discussion for a more detailed description of each model.